Flow-Dependent Vascular Heat Transfer during Microwave Thermal Ablation

Jason Chiang, Kieran Hynes, Christopher L. Brace, *Senior Member, IEEE*

Abstract— **Microwave tumor ablation is an attractive option for thermal ablation because of its inherent benefits over radiofrequency ablation (RFA) in the treatment of solid tumors such as hepatocellular carcinoma (HCC). Microwave energy heats tissue to higher temperatures and at a faster rate than RFA, creating larger, more homogenous ablation zones. In this study, we investigate microwave heating near large vasculature using coupled fluid-flow and thermal analysis. Low-flow conditions are predicted to be more likely to cause cytotoxic heating and, therefore, vessel thrombosis and endothelial damage of downstream tissues. Such conditions may be more prevalent in patient with severe cirrhosis or compromised blood flow. High-flow conditions create the more familiar heat-sink effect that can protect perivascular tissues from the intended thermal damage. These results may help guide placement and use of microwave ablation technologies in future studies.**

I. INTRODUCTION

Thermal tumor ablation has emerged as a treatment option for patients who are ineligible for surgery or have unresectable solid tumors [1]. Ablation procedures can be performed percutaneously and are associated with less bleeding, quicker recovery and virtually no scarring compared to surgery. The primary approach of ablative therapies is to create enough thermal stress to cause cellular necrosis. Immediate cell death occurs when tissue temperatures reach 52°C, while temperatures from 43-52°C can cause cell death when maintained for longer periods of time [2].

Radiofrequency (RF) electrical current remains the most widely used heat generation source for thermal ablation. However, RF ablation is a self-limiting process since ablative temperatures lead to water vaporization and dehydration, which in turn increase impedance to electrical current flow [3]. Such limited heating also makes RF ablation susceptible to the "heat sink" effect of nearby blood vessels [4]." Large vascular heat sinks cause suboptimal perivascular heating and increased risk for tumor recurrence in patients undergoing RF ablation [5]. Microwave energy,

on the other hand, propagates through all types of non-metallic material, including the dehydrated, charred and desiccated tissues associated with thermal ablation zones. As a result, continuous powers can be applied during microwave ablation, leading to larger and more complete ablation zones compared to RFA [6].

A consequence of using continuous high powers, however, is the possibility of transferring energy through nearby vessels during an ablation procedure. Microwave heating has been shown to be capable of overcoming vascular heat sinks, but little is known about how microwaves transfer heat into the nearby vasculature. Therefore, there is concern that very high powers could lead to greater risk of vascular damage and subsequent complications (Figure 1A and 1B). Concerns of vascular thrombus following RF ablation procedures were limited because of their low incidence and tendency to self-resolve over time [7]. As a result, there have only been a few studies looking at the theoretical heat transfer of thermal ablations [8]. However, with the recent development of microwave ablation, there have already been reports of thermal damage in peri- and intravascular areas outside of the ablation zone, leading to portal vein thrombosis [9]. Portal vein thrombosis and associated elevated portal vein pressure are linked with high risks of variceal bleeding and decreased liver perfusion, which can be life-threatening for
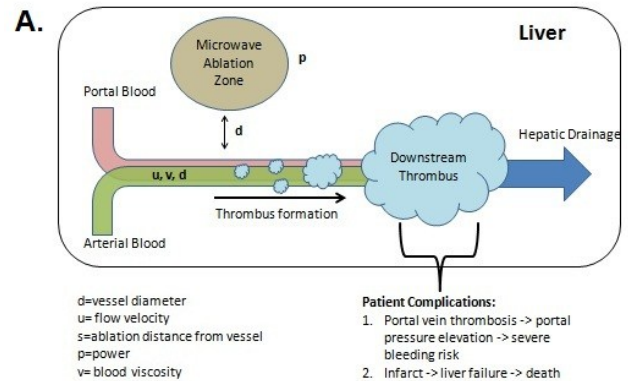

Figure 1. A) Potential of cytotoxic heat transfer in microwave tumor ablations near vessels. B) Thrombus formation during an-vivo study of high-powered microwave ablation

patients already suffering from compromised liver reserves. As more clinical centers worldwide adopt microwave ablation technology, and treatment approach becomes more aggressive, improved understanding of vascular heat transfer is necessary.

In this study, we employ finite-element modeling to investigate the potential of cytotoxic heat transfer in blood vessels near high-temperature ablation zones. Simulations were validated in a phantom vessel model and used to identify conditions that favor vascular damage or thrombosis.

II. METHODS

A) Numerical Modeling

We utilized the finite-element software COMSOL (v3.5) to generate a model that coupled heat transfer with fluid flow analysis. Our geometry was set up in a three-dimensional domain with a heat source placed 1-3 cm away from a liver-embedded blood vessel of 1 cm diameter. Liver tissue properties were taken from available literature [10]. We utilized the incompressible Navier-Stokes model to simulate the laminar flow conditions inside a blood vessel. The relation of the aforementioned variables in a vessel is as follows:

$$\rho \frac{\partial u}{\partial t} + \rho(u \cdot \nabla)u = \nabla \cdot [-\rho I + \eta(\nabla u + (\nabla u)^T)] \quad (1)$$

$$\nabla \cdot u = 0 \quad (2)$$

Variable η is the dynamic viscosity of the blood and velocity u is the dependent variable which is then inserted into the conduction-convection equation as an input. We assumed blood to be a Newtonian fluid with no temperature-dependence in order to simplify the computation. This is a valid assumption at ablation temperatures since blood viscosity converges to a steady-state value at above-physiological temperatures. To model the thermal energy propagation through the tissue and vessel in from the ablation zone, we utilized a convection/conduction equation,

$$\rho c_\rho \frac{\partial T}{\partial t} + \nabla \cdot (-k\nabla T) = Q - \rho C_\rho u \cdot \nabla T \quad (3)$$

The variable ρ is the density, C_ρ is the heat capacity, Q is the heat source and u is the velocity. The heat source Q is given in W/m^3 and empirically determined beforehand to match up with the heating powers associated with microwave applicator probes. In this case, we used 10^7 W/m^3, which provided a heating pattern similar to that created by a monopole microwave applicator delivering 50 watts of power for 2 minutes.

To observe the effect ablation spacing, we first varied the distance of the heating source from the vessel from 1 cm to 3cm. Temperature profiles along the vessel were calculated and compared to each other. To observe the effect of flow velocity, we varied the velocity from 1 mm/sec to 1000 mm/sec on a logarithmic scale. These values encompass all possible flow ranges seen in healthy and diseased liver vasculatures of the portal-venous system [11]. Temperature profiles in a spatial domain were determined and a cytotoxic damage zone was determined by highlighting the 53°C isotherm shell, which was associated with immediate cytotoxicity.

B) Experimental validation with phantom vessel

An agar phantom model was used to validate the numerical modeling while introducing complexities that reflect a more clinical environment. An agar vessel phantom had advantages over ex-vivo tissue in that it was homogenous and devoid of vessels with complex geometries. Furthermore, our agar vessel was semi-transparent, which facilitated precise antenna placement. Lastly, the agar vessel phantom was reproducible and could reliably create an idealized environment for comparisons with simulations. A clinical microwave ablation system (Neuwave Medical, USA) was used to create an ablation zone 1 cm away from the vessel in the transverse direction. Fiber-optic temperature probes (Neoptix, Canada) were inserted inside the vessel to line up ipsilaterally with the ablation probe. The position inside the vessel allowed us to more accurately measure the heat transfer from the ablation zone. The vessel phantom on one end was connected to a flow pump (Masterflex, USA) to deliver fluid through the vessel. Our computational model assumed a Newtonian fluid input and thus we chose to use water for validation purposes. The flow pump was set to deliver blood at rates associated with cytotoxic heat transfer found in our numerical models.

The ablations were made at 50 W for 5 minutes and temperatures were recorded real-time at a rate of 1 Hz during the entire ablation period at 0, 2, 4 and 6 cm downstream from the ablation zone. A 1 cm vessel diameter was selected to accommodate the temperature probes without disrupting the fluid flow during the ablation.

III. RESULTS

A) Numerical Modeling Results

The numerical models predicted decreased heating along the vessels at all velocities when the heating source was moved from 1 cm to 3 cm away from the vessel (Figure 2A). Placing the applicator further away from the vessel was more effective in decreasing the temperature distribution as the vessel velocities became slower. At a velocity of 0 mm/sec, 1 mm/sec and 5 mm/sec, there was a drop in max temperature from 119°C to 57°C, 76°C to 48°C and 50°C to 40°C, respectively. There was also a decrease in downstream heating as the applicator was moved further away. With the applicator placed 1 cm from the vessel, the 1 mm/sec blood velocity carried heat higher than 53°C, where immediate cytotoxicity occurs, up to 5 cm downstream of the heating source. With the 3 cm spacing, under the same blood
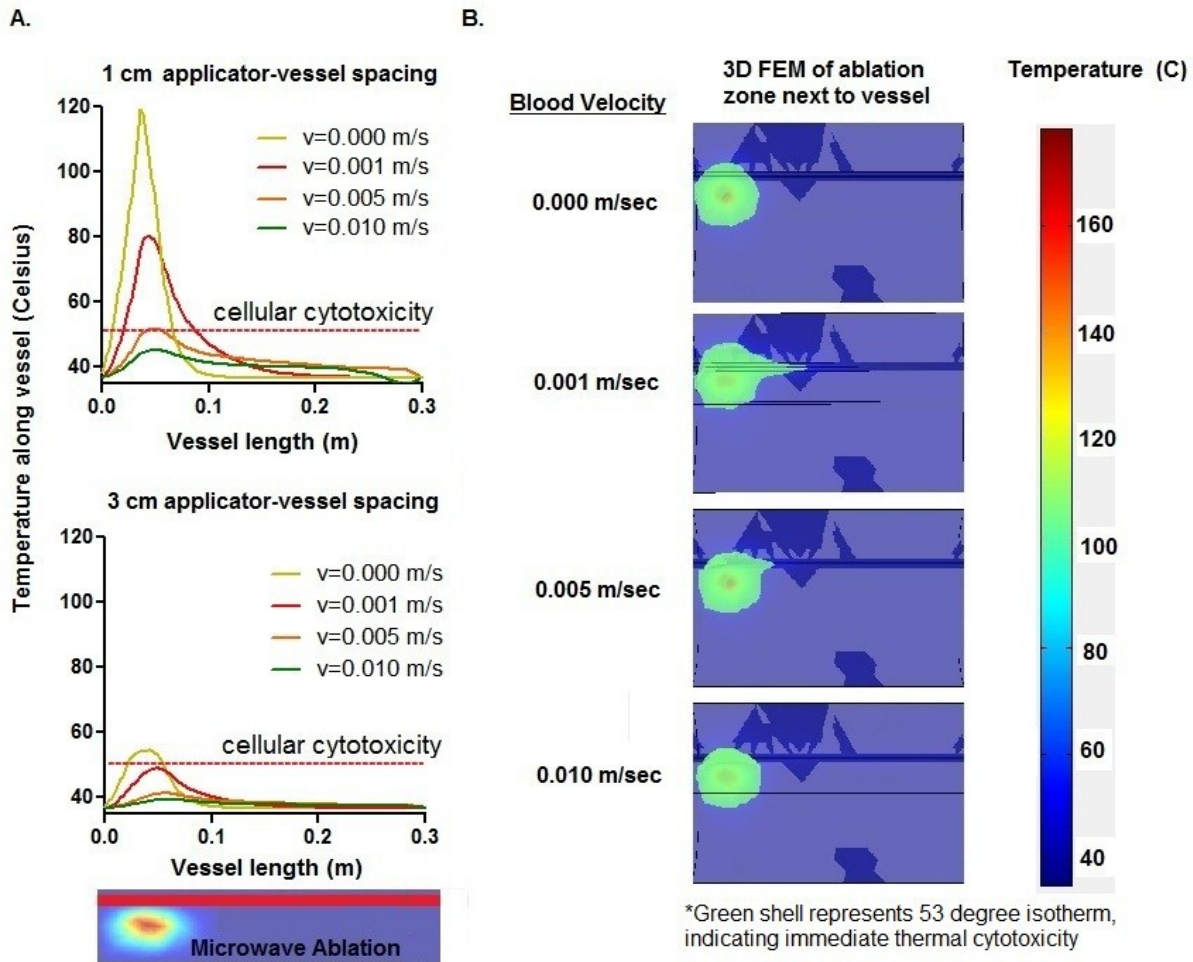
Figure 2. Numerical results depicting decreased heat transfer while increasing distance between applicator and vessel from A) 1 cm to 3 cm. B) Temperature map of ablation at different velocities, with the 53°C isotherm highlighted to indicate location of immediate cellular necrosis. Increasing blood velocity is associated with a decrease in intravascular heat transfer near ablation zones.

velocity, the temperature does not rise higher than 53°C at any point past the heating source.

With respect to blood velocity, the model demonstrated a negative correlation between flow rates and downstream heating. However, this correlation did not hold at the null velocity, where there was virtually no downstream heating past the applicator. In this no-flow condition, the ablation zone was confined only to the treatment region by conductive heat transfer. In the low-flow conditions (1-5 mm/sec), significant downstream heating occurred, with temperatures rising above 53°C up to 5 cm past the heating source. As we move to faster velocities (5-10 mm/sec), there is less heat being carried downstream and temperature does not rise substantially over that of a normal vessel (Figure 2B). At these faster velocities, the heat distribution behaved similarly to that of a vessel acting as a heat sink. This pattern suggests that the flow is fast enough to dissipate energy over long distances rather than local heating downstream tissues.

B) Phantom Validation Results

The temperature trends in the phantom validation were similar to those found in the computational simulations

(Figure 3). At higher blood velocities (11-14 mm/sec), there was no appreciable rise in temperature along the vessel (6 cm). However, once a lower velocity was reached (3 mm/sec), there was a significant increase in temperature inside the vessel as the energy deposit started accumulating. At this lower velocity, the temperature was significantly higher compared to the other 3 velocities at locations 4 and 6 cm downstream from the heating zone ($p<0.05$ at 4 cm, $p<0.02$ at 6 cm). There was no significant difference in temperature elevations converged as we moved closer and closer to the actual ablation probe location, which was expected from the volumetric heating associated with microwave antennas.

IV. DISCUSSION

This study investigated the risk of vascular damage during microwave thermal ablation. As expected, vascular heating decreased as distance between the vessel and thermal source increased, regardless of fluid velocity. This suggests that distant microwave antenna placement is a feasible way to reduce the risk of vascular heating, downstream damage and thrombosis during microwave tumor ablation.

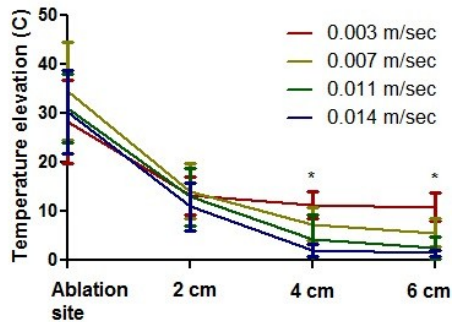## Intravascular Temperature Elevation Along Vessel During Ablation

Figure 3. Phantom modeling results (n=6) demonstrating significantly higher temperature elevation (p<0.05) at 0.003 m/sec compared to all other perfusion rates at vessel locations 4-6 cm downstream from the ablation zone.

We noted a rapid increase in cytotoxic heat transfer in vessels with decreased perfusion, notably at velocities of 7 mm/s or less. At higher velocities, the thermal heat transfer occurs too rapidly for localized temperature elevations. The phantom vessel modeling results confirmed significant temperature elevations found in the numerical modeling study. This finding is potentially relevant for potential ablation patients, notably those who suffer from pre-existing cirrhotic livers and poor vascular flow. These implications suggest that characterization of nearby vessel size and blood flow should be taken into account during the treatment planning stage. The scale-invariant nature of the Navier Stokes equations imply that the computational results can be translatable to various vessel sizes and flow velocities associated with a variety of patient profiles during an ablation procedure.

The velocities encountered in these simulations and models are considered low, even for the smaller vasculature in a cirrhotic liver. This discrepancy suggests that there are perhaps other velocity-dependent factors involved in the heat transfer process beyond simple conduction-convection. One possibility is the formation of water vapor inside the vessel from surrounding tissue, which has been seen in ex-vivo and in-vivo ablation studies. Efforts to account for water vapor formation inside heated vessels have been investigated previously and can potentially be coupled to our numerical models to predict heat transfer in a more clinically realistic scenario[12-13].

Assessing the performance of our numerical modeling in predicting clinical thrombotic risk is critical. However, there are aspects that have not yet been integrated into the numerical model, such as the potential non-Newtonian behavior of blood at high temperatures, effects of heating on the clotting cascade, as well as the tortuous vessel geometries encountered in liver anatomy. We addressed some of these issues through our phantom vessel model, which offered an idealized vessel geometry that could validate our simplified numerical model. We added additional complexities such as utilizing a clinical microwave ablation system but recognize

that there are still gaps between our numerical/phantom model and the clinical scenario. However, the similarities in trend and temperature elevation between the numerical and phantom modeling suggests that our numerical modeling is a viable starting point to creating a thrombotic risk model. Integrating more complexities into our numerical models may provide more accuracy and clinical utility for future studies.

V. CONCLUSION

Creating ablation zones near vessels with slow blood flow can potentially increase the risk of vascular damage and thrombosis. Further investigation to determine the optimal placement of the microwave antennas to nearby blood vessels appears warranted, and may guide treatment planning in future studies.

REFERENCES

[1] C. L. Brace, "Microwave tissue ablation: biophysics, technology, and applications," *Crit Rev Biomed Eng*, vol. 38, no. 1, pp. 65–78, 2010.
[2] S. Pisa, M. Cavagnaro, P. Bernardi, and J. C. Lin, "A 915-MHz antenna for microwave thermal ablation treatment: physical design, computer modeling and experimental measurement," *IEEE Trans Biomed Eng*, vol. 48, no. 5, pp. 599–601, May 2001.
[3] C. L. Brace, P. F. Laeseke, L. A. Sampson, T. M. Frey, D. W. van der Weide, and F. T. Lee, "Microwave Ablation with Multiple Simultaneously Powered Small-gauge Triaxial Antennas: Results from an in Vivo Swine Liver Model1," *Radiology*, vol. 244, no. 1, pp. 151 –156, Jul. 2007.
[4] C. L. Brace, "Radiofrequency and microwave ablation of the liver, lung, kidney, and bone: what are the differences?," *Curr Probl Diagn Radiol*, vol. 38, no. 3, pp. 135–143, Jun. 2009.
[5] D. S. K. Lu, S. S. Raman, D. J. Vodopich, M. Wang, J. Sayre, and C. Lassman, "Effect of vessel size on creation of hepatic radiofrequency lesions in pigs: assessment of the 'heat sink' effect," *AJR Am J Roentgenol*, vol. 178, no. 1, pp. 47–51, Jan. 2002.
[6] Y. K. Cho, H. Rhim, and S. Noh, "Radiofrequency Ablation versus Surgical Resection as Primary Treatment of Hepatocellular Carcinoma Meeting the Milan Criteria: A Systematic Review," *J Gastroenterol Hepatol*, Jun. 2011.
[7] N. C. Yu, S. S. Raman, Y. J. Kim, C. Lassman, X. Chang, and D. S. K. Lu, "Microwave liver ablation: influence of hepatic vein size on heat-sink effect in a porcine model," *J Vasc Interv Radiol*, vol. 19, no. 7, pp. 1087–92, Jul. 2008.
[8] A. Orlacchio, A. Mancini, G. Calabrese, F. Bolacchi, V. Cozzolino, M. Angelico, and G. Simonetti, "Portal vein thrombosis after radiofrequency ablation of HCC," *Minerva Gastroenterol Dietol*, vol. 56, no. 1, pp. 87–91, Mar. 2010.
[9] M. Akahane, H. Koga, N. Kato, H. Yamada, K. Uozumi, R. Tateishi, T. Teratani, S. Shiina, and K. Ohtomo, "Complications of percutaneous radiofrequency ablation for hepato-cellular carcinoma: imaging spectrum and management," *Radiographics*, vol. 25 Suppl 1, pp. S57–68, Oct. 2005.
[10] T.-M. Chen, P.-T. Huang, L.-F. Lin, and J.-N. Tung, "Major complications of ultrasound-guided percutaneous radiofrequency ablations for liver malignancies: single center experience," *J Gastroenterol Hepatol*, vol. 23, no. 8 Pt 2, pp. e445–50, 2008.
[11] O. E. Owen, F. A. Reichle, M. A. Mozzoli, T. Kreulen, M. S. Patel, I. B. Elfenbein, M. Golsorkhi, K. H. Chang, N. S. Rao, H. S. Sue, and G. Boden, "Hepatic, gut, and renal substrate flux rates in patients with hepatic cirrhosis," *J. Clin. Invest.*, vol. 68, no. 1, pp. 240–252, Jul. 1981.
[12] D. Yang, M. C. Converse, D. M. Mahvi, and J. G. Webster, "Expanding the bioheat equation to include tissue internal water evaporation during heating," *IEEE Trans Biomed Eng*, vol. 54, no. 8, pp. 1382–8, 2007.
[13] Z. Ji and C. L. Brace, "Expanded modeling of temperature-dependent dielectric properties for microwave thermal ablation," *Phys Med Biol*, vol. 56, no. 16, pp. 5249–5264, Aug. 2011.